NANO LETTERS

Letter

Scanning Tunneling Microscopy Images of Alkane Derivatives on Graphite: Role of Electronic Effects

Boaz Ilan, Gina M. Florio, Mark S. Hybertsen, B. J. Berne, and George W. Flynn

Nano Lett., **2008**, 8 (10), 3160-3165 • DOI: 10.1021/nl8014186 • Publication Date (Web): 18 September 2008

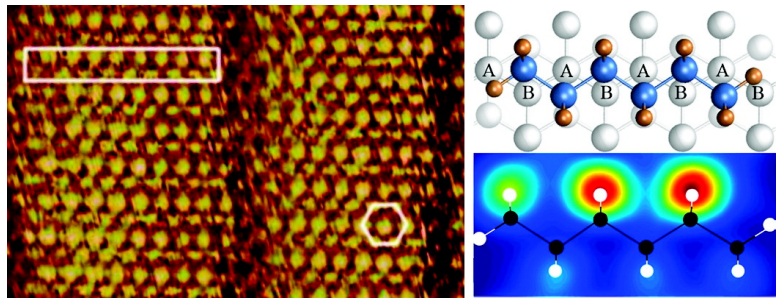

NANO LETTERS

2008
Vol. 8, No. 10
3160-3165

Scanning Tunneling Microscopy Images of Alkane Derivatives on Graphite: Role of Electronic Effects

Boaz Ilan,[†,‡] Gina M. Florio,[‡,§] Mark S. Hybertsen,[*,||] B. J. Berne,[*,†] and George W. Flynn[*,†,‡]

Department of Chemistry, Center for Electron Transport in Molecular Nanostructures, Columbia University, New York, New York 10027, Department of Chemistry and Department of Physics, St. John's University, Queens, New York 11439, and Center for Functional Nanomaterials, Brookhaven National Laboratory, Upton, New York 11973

Received May 16, 2008; Revised Manuscript Received August 29, 2008

ABSTRACT

Scanning tunneling microscopy (STM) images of self-assembled monolayers of close-packed alkane chains on highly oriented pyrolitic graphite often display an alternating bright and dark spot pattern. Classical simulations suggest that a tilt of the alkane backbone is unstable and, therefore, unlikely to account for the contrast variation. First principles calculations based on density functional theory show that an electronic effect can explain the observed alternation. Furthermore, the asymmetric spot pattern associated with the minimum energy alignment is modulated depending on the registry of the alkane adsorbate relative to the graphite surface, explaining the characteristic moiré pattern that is often observed in STM images with close packed alkyl assemblies.

Scanning tunneling microscopy (STM) is widely used to characterize the structure of molecular self-assembled monolayers on surfaces such as graphite. On the basis of the assignments of the constituent molecular motifs, the two-dimensional phases of the assembled structures are identified.[1−3] Because of the accessibility of this system using STM probes, the technique is widely utilized to study model systems that elucidate fundamental driving forces in self-assembly.[3−9] Very often the structural assignment is based on simply overlaying plausible molecular models onto the STM images. However, the clean graphite surface itself is one of the prototypical examples of the role that electronic effects can play in an STM image, where only every second atom appears under typical scan conditions.[10,11] This has been explained by the impact of the electronic coupling between the layers of carbon sheets in graphite. The states near the Fermi energy are dominated by π-electrons on the B-type carbon atoms of the surface that do not have a neighbor atom immediately below them in the normal graphitic lattice.[12]

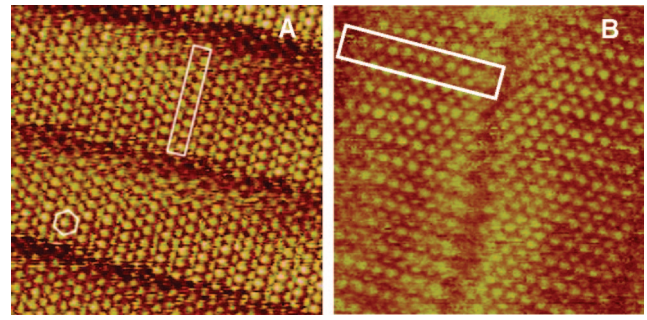

Figure 1. Topographic (constant current) STM images of (A) nonadecane ($C_{19}H_{39}$) and (B) 1-bromoeicosane ($C_{20}H_{41}Br$) at the liquid-graphite interface. The white boxes indicate the approximate location of a single molecule. (A) Image has dimensions of 7.5 nm × 7.5 nm and was recorded at a bias of −1.5 V, setpoint current of 300 pA, and a scan rate of 6.78 Hz. (B) Image has dimensions of 6 nm × 6 nm and was recorded at a bias of −1.50 V, setpoint current of 250 pA, and a scan rate of 7.629 Hz. Each solution was prepared at half-saturation in 1-phenyloctane for nonadecane and octanoic acid for 1-bromoeicosane.

Interestingly, these electronic effects have been observed to affect images of adsorbates such as benzene.[13,14] Many of the molecules considered in studies of self-assembly include long alkyl arms. A survey of papers shows that the image of the arms is often asymmetric.[1,15−26] Two examples from our experiments illustrate this effect in Figure 1. The alternating rows of bright and dark spots evidently correspond

* Authors to whom correspondence should be addressed. (M.S.H.) Phone: 631-344-5996. E-mail: mhyberts@bnl.gov. (G.W.F.) Phone: 212-854-4162. E-mail: gwf1@columbia.edu. (B.J.B.) Phone: 212-854-2186. E-mail: bb8@columbia.edu.

† Department of Chemistry, Columbia University.

‡ Center for Electron Transport in Molecular Nanostructures, Columbia University.

§ St. John's University.

|| Brookhaven National Laboratory.

10.1021/nl8014186 CCC: $40.75
Published on Web 09/18/2008

to the top rows of hydrogen atoms. Furthermore, the asymmetry often exhibits longer range modulation. Does this asymmetry indicate physical rotation of the alkane, with potential impact on understanding the assembled structure? Alternatively, does it have an electronic origin?

A tilt of the alkane backbone with respect to the graphite surface could account, in principle, for the alternating bright-dark spot pattern. However, recent classical molecular dynamics (MD) simulations of *n*-hexane[6,27] and 1-bromoeicosane ($C_{20}H_{41}Br$)[28] assemblies on HOPG show no out of plane tilting of the backbone skeleton with respect to the graphite surface in the stable phases. In this paper, we use density functional theory based calculations of alkane molecules on graphite to investigate a possible electronic origin for this asymmetric spot pattern. Our calculations show that the observed asymmetric pattern can be induced by coupling of the frontier orbitals of the alkane to the nonequivalent carbons of type A and B of the substrate associated with the ABAB stacking of the graphite lattice. This coupling depends on the registry of the alkane chain relative to the parallel C−C chain of the graphite layer, showing distinct modulations, including even phase reversals in the image. These results give a natural interpretation of the images shown in Figure 1, as well as many similar cases in the literature.[1,15−26]

We have used STM to study close-packed assemblies of n-alkanes (here nonadecane ($C_{19}H_{39}$)) and functionalized alkane derivatives (here 1-bromoeicosane) on graphite. Solutions were prepared at half-saturation concentration in 1-phenyoctane for nonadecane and octanoic acid for 1-bromoeicosane. Images were typically recorded at the graphite/solvent interface under conditions of −1.50 V bias and a setpoint current of 250 pA. Typical images are depicted in Figure 1A,B for nonadecane and 1-bromoeicosane, respectively. The molecular backbone-trough angle of the ordered monolayer is approximately 90°, and the interchain distance is approximately 4.4 Å. Assignment of the fundamental molecular unit in the assembly is indicated by the white boxes. The prominent features form a triangular network, but the intensity of the features alternates in rows. These features are assigned to the positions of hydrogen atoms, since the electron density is dominated by the protruding hydrogen atoms.[29] The characteristic hexagonal signature (sketched hexagon in Figure 1A) suggests that the backbone skeleton of the alkanes is, at least approximately, parallel to the graphite surface.

Molecular dynamics (MD) calculations were performed according to the classical all atom optimized potential for liquid simulations (OPLS-AA)[30] for the inter- and intrachain interactions using the simulation (SIM) package.[31] The interactions of the atoms of the chains with the graphite lattice are described by a Lennard-Jones potential[32] in combination with an image charge interaction term. The calculations were carried out without periodic boundary conditions under vacuum conditions. Explicit solvent effects have been examined in a separate study.[28] First principles calculations were performed using the ab initio Siesta[33] program within the local density approximation (LDA) to

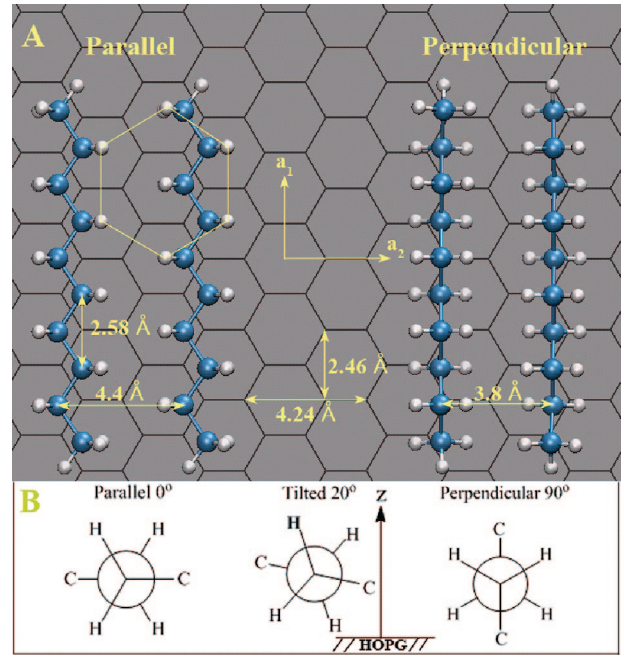

Figure 2. (A) The backbone skeletons of the left and right pairs of chains lie parallel and perpendicular to the graphite lattice, respectively. a_1 and a_2 are the principal and secondary graphite lattice vectors, respectively. (B) From left to right: Newman projections corresponding to the parallel, tilted, and perpendicular orientations of the backbone skeleton of the alkane chain.

density functional theory (DFT).[34−36] Norm-conserving Troullier-Martins pseudopotentials[37] were used with an efficient numerical orbital, double-ζ plus polarization (DZP) basis and a very fine sampling of the surface Brillouin Zone by a Monhorst-Pack grid.[38] The model systems studied in this paper consist of hexane and decane molecules on top of two monolayers of graphite with periodic boundary conditions. Although started from an energy minimized OPLS MD structure, the hexane and decane molecules were relaxed again with the graphite atoms kept fixed. Using the electronic states from the Siesta calculation, a simulated STM image is calculated based on the Tersoff-Hamann analysis at a constant height.[39] Further details of the theoretical procedures are described in the Supporting Information.

A model of commensurate registry along the [010] vector of the graphite lattice (a_2 vector in Figure 2A) has been proposed by Groszek based on adsorption isotherm experiments of long n-alkanes from solution, long before the advent of STM studies.[40] Groszek's model implies a uniaxial compression of the monolayer by more than 10% relative to the alkane molecular crystal structures. On the basis of X-ray measurements of triclinic three-dimensional (3D) alkane crystals[41] the interchain distance is ∼4.8 Å (defined perpendicular to the chain axis within the plane containing the backbone skeleton). The corresponding distance between carbon rows of the graphite lattice is ∼4.24 Å. Groszek's model assumes that the chains are lying parallel to the graphite surface. Two distinct (parallel and perpendicular) packing motifs are illustrated for pairs of decane molecules (Figure 2A). The pairs of molecules shown were energy minimized according to the classical OPLS force field

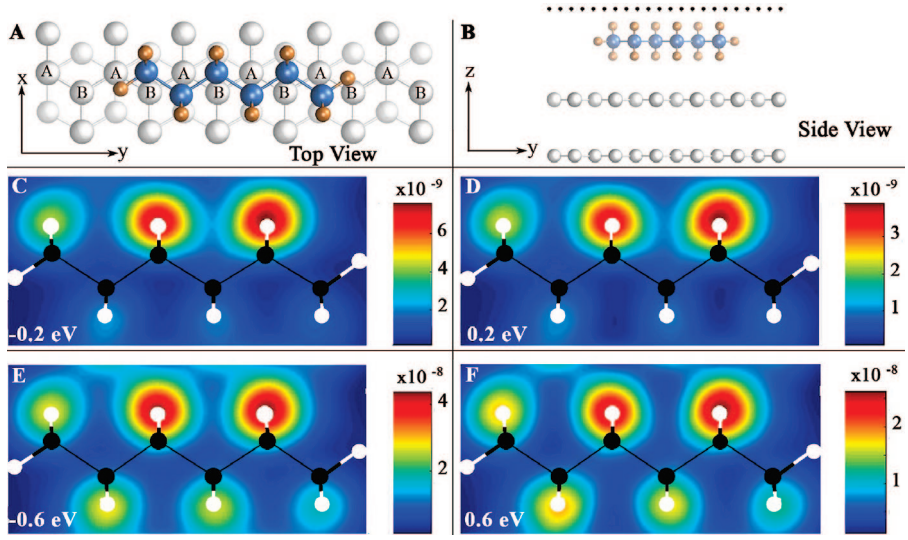

Figure 3. Top and side views of the model system are depicted in (A) and (B), respectively. The cut-plane (dotted line) is sketched schematically in (B). Two rows of A and B carbon atoms of the top layer of the graphite lattice are sketched in panel A. The simulated STM image on the cut-plane at bias voltages −0.2, 0.2, −0.6, and 0.6 eV are depicted in (C−F), respectively (units electrons per cubic bohr). The black and white circles indicate, respectively, the projection of the carbon and hydrogen atoms of the hexane molecule onto the *xy* plane.

without periodic boundary conditions. The left pair of chains lie with their (zigzag) backbone skeletons (all-trans configuration) parallel to the graphite surface. The backbone skeletons of the right pair of chains in Figure 2A are perpendicular to the graphite surface. Steric considerations require the terminal C−C vectors of the right pair of chains to orient in opposite directions suggesting a highly selective transition pathway between the parallel and perpendicular configurations. The total potential energies of the two pairs of parallel and perpendicular configurations are −47.8 and −42.1 kcal/mol, respectively, favoring the parallel configuration. Note, however, that the energetics for a full layer must take into account the different surface coverages of the parallel and perpendicular motifs. Evidence for both perpendicular and parallel orientations of the backbone skeleton has been seen both in early STM[42] and in neutron diffraction[43] studies of self-assembly for alkane derivatives on graphite. This suggests that at least a finite fraction of the orientations may be perpendicular, perhaps in order to fulfill the condition for registry. However, the hexagonal signature observed in the STM images (Figure 1) is clearly identifiable with the arrangement of the hydrogen atoms of the left pair of chains in Figure 2A, but not the pair on the right. The hydrogen atoms of the left (parallel) pair of chains in Figure 2A are approximately positioned on top of the centers of graphite hexagons.

The calculated interchain distance for the parallel chains (left pair in Figure 2A), ∼4.4 Å, is significantly reduced from the bulk value. The corresponding distance for the perpendicularly oriented backbone skeletons (right pair in Figure 2A), 3.8 Å, is smaller than the corresponding graphite lattice spacing, ∼4.24 Å. These values suggest that the alternating bright-dark spot pattern could indicate, in principle, an out-of-plane tilting of the backbone skeleton with respect to the graphite surface (rotation about the chain axis). Such a tilting (the topmost hydrogen atom (bold font) in the tilted Newman projection of Figure 2B) is expected to reduce the average interchain distance of the parallel arrangement, allowing the ordered monolayer to draw closer to commensurability with the graphite lattice. In a separate study, the subtle competition between corrugation of the surface potential (driving commensurability) and the interchain interactions were evaluated through classical MD simulations, including the role of solvent effects. The results indicate that the tilted orientations are unstable (under both vacuum and explicit solvent conditions). The tilted orientations have been observed to relax back to either a parallel or perpendicular orientation depending on whether the out-of-plane tilt angle of the starting configurations was less than or larger than 45°, respectively.[28]

On the basis of the hexagonal arrangement of the top hydrogen atoms observed in the STM images in Figure 1 and the classical MD results, we set up our DFT calculations using the Groszek model with perfect registry with respect to the graphite lattice (along the a_2 axis in Figure 2A). This assumption allows us to model simply both the graphite lattice and the alkane molecules using the same periodic boundary conditions. The periodically replicated alkane chains form a close packed assembly. In addition, the registry provides an additional test of whether commensurability forces the backbone skeletons to buckle out of the graphite plane. The setup of the composite hexane + graphite system is depicted in Figures 3A (top view) and 3B (side view). The backbone skeleton of the relaxed hexane molecule lies perfectly parallel to the graphite surface (Figure 3B). The relaxed hexane molecule therefore does not exhibit out-of-plane tilting despite the imposed commensurability along the *x*-axis. Along the chain axis, the distance between second nearest neighbor carbon atoms, ∼2.53 Å, is slightly larger than the corresponding distance in the graphite lattice, ∼2.46 Å (the corresponding distance in the classically minimized configuration (Figure 2) is ∼2.58 Å).

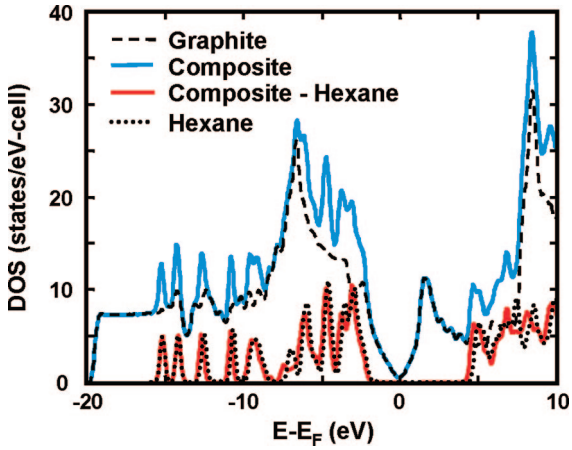

Figure 4. The total density of states is depicted for four components of the model system: (1) graphite (two monolayers); (2) composite system (graphite + hexane); (3) difference between composite system and graphite; and (4) hexane (with periodic boundary conditions.)

The density of states (DOS) for the case of hexane on graphite (here two layers only) is depicted in Figure 4. For comparison, the bare graphite DOS is also shown, as well as a representation of the hexane orbital energies, calculated for a periodic array of molecules in the same unit cell. The coordinates of the minimized hexane (from the composite system) were used for the latter calculation. The difference between the composite system DOS and the graphite DOS is essentially identical to the orbital energy distribution of the hexane molecules. As one would expect, the DFT calculations show that the alkane electronic states are weakly perturbed by coupling to the graphite surface. The close alignment of the DOS for the bare graphite and the composite system in the vicinity of E_F imply minimal charge transfer between hexane and graphite.

We now use the electronic states from the commensurate calculation to analyze the STM images, returning to the registry issue again below. The simulated STM images, at a cut plane parallel to the graphite surface (~1.6 and ~5.0 Å above the top hydrogen atoms and top graphite layer, respectively) are displayed in Figure 3, panels C−F, for bias voltages of −0.2, 0.2, −0.6, and 0.6 eV, respectively. The projected positions of the carbon and hydrogen atoms of the hexane molecule are depicted in Figure 3C−F by black and white circles, respectively. The simulated STM images for bias voltages −0.2 and 0.2 eV (Figure 3C,D, respectively) clearly display a strong asymmetry of the intensity between the top two rows of hydrogen atoms, as observed in the experiments. The origin of the asymmetry is due to electronic structure effects since all the top hydrogen atoms are approximately at the same height with respect to the graphite lattice (Figure 3B). Notice (Figure 3A) that the rows of the nonequivalent *A* and *B* carbons of the graphite lattice lie parallel to the rows of the hydrogen atoms. The asymmetry is qualitatively independent of polarity. Quantitatively, however, the total magnitude of the simulated STM image is approximately twice as large for the negative relative to positive polarity (at the same absolute value of the bias voltage - see Figure 3, panel C versus panel D and Figure 3, panel E versus panel F). The asymmetry smoothes out with increasing magnitude of the bias voltage (Figure 3E,F), approximately vanishing at bias voltages of ±1 V (not shown). The magnitude of the calculated bias voltage at which the asymmetry vanishes is expected to increase by a factor of ~2 with the inclusion of additional layers of graphite. We have also verified that the asymmetry does not manifest itself for hexane on top of a single monolayer of graphite.

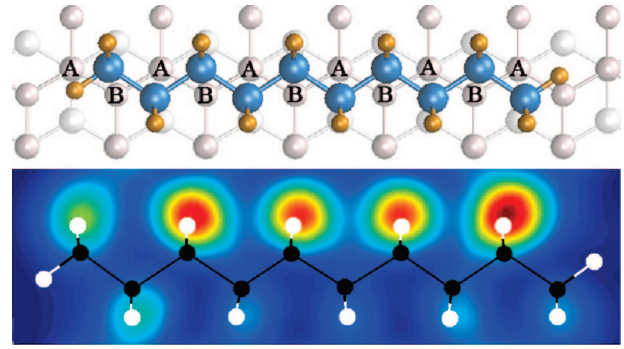

Figure 5. The relaxed decane system and the corresponding simulated STM image at a bias voltage of −0.2 eV. The maximum amplitude of the simulated STM image (not shown) is ~8 × 10^{-9} (units electrons per cubic bohr).

The image contrast appears to be modulated along the direction parallel to the chain axis (Figure 3). To further investigate this feature we performed an analogous calculation for a decane molecule on top of two layers of graphite. The relaxed configuration and the corresponding simulated STM image at a bias voltage of −0.2 eV are depicted in Figure 5. The simulated STM image of the decane molecule supports the trend seen for the hexane molecule in that the image contrast is not uniform along the chain axis. Such modulations of the image contrast have been observed in our experiments (Figure 1) and reported in the literature.[1,15−26]

The HOMO level of the hexane molecule is clearly closer to E_F relative to the LUMO level (Figure 4). Does this imply that the occupied frontier alkane states dominate the images? We analyzed projections of the wave functions of the composite system near E_F onto the hexane frontier molecular orbitals. These projections showed contributions from several occupied *and* empty frontier orbitals. The local atomic orbital combinations on the methylene subunits that contribute to the STM image consist of two basic types (see coordinate system in Figure 3): carbon p_z orbitals coupled to an odd combination of the hydrogen s orbitals, and carbon p_x and s orbitals coupled to an even combination of the hydrogen s orbitals. Bonding combinations comprise the occupied frontier orbitals on the alkane chains while antibonding combinations form the empty frontier orbitals. Each set shows a dispersion of a few eV that reflects the internal electronic coupling within the chain. The graphite wave functions near E_F have most of their weight on the carbon p_z orbitals of the B type atoms in Figure 3A. These clearly couple most strongly to every other methylene unit. The tail of the wave function, sensed by the STM, is determined by coupling of the alkane frontier orbitals to the graphite

$$\left|\psi\right\rangle = \left|\psi_{Gr}\right\rangle + \sum_{Alk}\left|\psi_{Alk}\right\rangle \frac{\langle\psi_{Alk}|\Delta V|\psi_{Gr}\rangle}{E_F - E_{Alk}} \quad (1)$$

First consider the limit in which the orbitals on the methylene subunits are weakly coupled to those on their neighbors. In this case, only those methylene orbitals close to the B type atoms will be coupled to the graphite wave functions near E_F, resulting in large contrast across the alkane backbone in the STM image. Second, consider the opposite limit in which the methylene orbitals are strongly coupled to those on their neighbors. In this case, the alkane frontier molecular orbital energies would exhibit large energy splittings. The relatively weak coupling of the graphite wave functions through the B type atoms would not be sufficient to disrupt the delocalization of the alkane HOMO, which would then dominate the image. As a result, the STM image would not show the type of contrast illustrated in Figure 3. In practice, the coupling between the orbitals on the methylene subunits is intermediate, as can be seen from the spread in the frontier orbital energies in Figure 4 over a scale of a few eV. Therefore, the STM images show partial contrast.

Now, we return to the commensurability question. Our MD simulations and STM experiments show that the alkane chains are in fact incommensurate with respect to the graphite lattice along the direction perpendicular to the chain axis. Furthermore, bulkier alkane derivates are even less likely to satisfy commensurability along this direction. In order to explore the impact of commensurability on the electronic asymmetry, we systematically shifted the periodic array of hexane chains in our DFT calculations through a full periodic cycle of registries with the graphite surface. As illustrated in Figure 6, we consider six choices of registry spaced by $a_o/2$ (a_o is the nearest neighbor distance of the graphite lattice). The case $\Delta x = 0$ corresponds to the global minimum configuration (Figure 3A). For the x-shifted configurations, the geometries were not further relaxed. The simulated STM images were calculated at the same cutoff plane ~1.6 Å above the top hydrogen atoms for a bias voltage of −0.2 eV (as in Figure 3C). An inversion of the asymmetric pattern is depicted between the global minimum configuration at $\Delta x = 0$ and the configuration at $\Delta x = a_o/2$ such that the bright-dark spot pattern is reversed. In addition, the asymmetry approximately vanishes at $\Delta x = -a_o$. This suggests that for incommensurate assemblies of alkane derivatives and other species with interdigitated alkyl arms, there will be systematic modulations in the observed contrast.

Local asymmetry in the images of alkane derivatives and alkyl groups is often observed in STM images in the literature.[1,15−26] The results of our calculations provide a natural explanation based on electronic effects. Furthermore, periodic modulations of the (local) asymmetric bright-dark spot pattern were clearly observed, for example, in high resolution STM images of a series of 1,3-disubstitued benzene alkyl molecules.[1] Although close packed, in the sense that each methylene is nestled in between two methylene units on the nearest chain, the observed moiré pattern suggests that these substituted alkyl molecules are not commensurate with the graphite lattice. The moiré

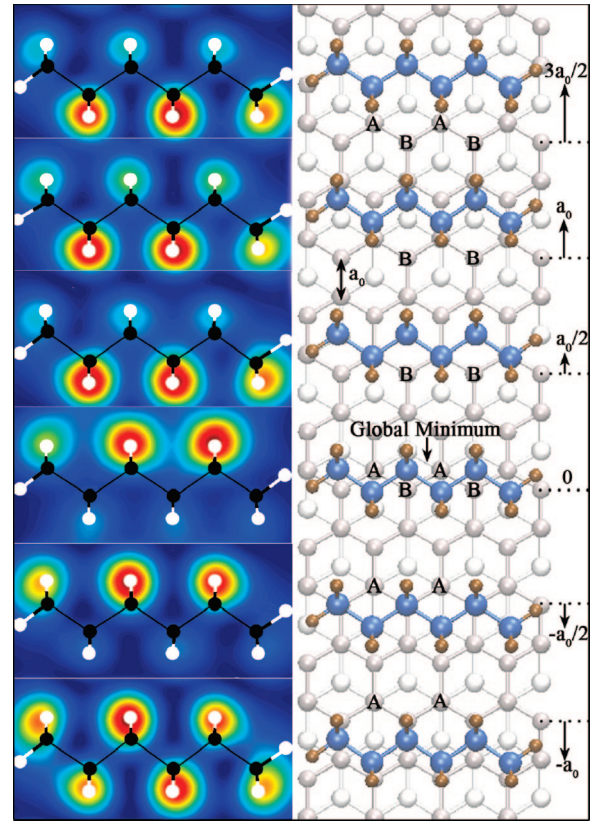

Figure 6. The simulated STM image at a bias voltage of −0.2 eV is depicted for successive shifts of the hexane molecule along the x-axis by multiples of $0.5a_o$. The carbon and hydrogen atoms of the hexane molecule are depicted by black and white circles, respectively. The corresponding configurations are depicted schematically on the right-hand side. The dotted lines correspond to positions of commensurability and the arrows depict the deviations from commensurability. The maximum amplitudes of the simulated STM images are approximately 3.3×10^{-8}, 3.2×10^{-8}, 7×10^{-9}, 7×10^{-9}, 1.3×10^{-8}, and 3.2×10^{-8} electrons per cubic bohr for $\Delta x = -a_o$, $-a_o/2$, 0, $a_o/2$, a_o, and $3a_o/2$, respectively.

patterns reported in refs 1 and 15−25 appear to display transitions between asymmetric and symmetric image contrasts as well as reversals of the asymmetric spot pattern in agreement with our calculations.

Note added. After completion of this paper, we became aware of a recently published DFT study of long-chain alkane assembly on graphite.[44] Their simulated STM image for polyethylene adsorbed with the backbone parallel to the graphite surface shows marked asymmetry in the apparent height of the hydrogen atoms, although they do not discuss the electronic origin of this effect.

Acknowledgment. We would like to thank Catalin D. Spataru, Mario G. Del Popolo, and Lorin Gutman for stimulating discussions. This work was supported by the National Science Foundation under Grants CHE-06-13401 and CHE-07-01483, by the Nanoscale Science and Engineering Initiative under Grant CHE-06-41523, by the New York State Office of Science, Technology, and Academic Research (NYSTAR), and by the U.S. Department of Energy, Office of Basic Energy Sciences, under Contract Nos. DE-AC02-98CH10886 and DE-FG02-88ER13937.

Supporting Information Available: This material is available free of charge via the Internet at http://pubs.acs.org.

References

(1) Plass, K. E.; Kim, K.; Matzger, A. J. *J. Am. Chem. Soc.* **2004**, *126*, 9042–9053.
(2) De Feyter, S.; De Schryver, F. C. *Chem. Soc. Rev.* **2003**, *32*, 139–150.
(3) Muller, T.; Werblowsky, T. L.; Florio, G. M.; Berne, B. J.; Flynn, G. W. *Proc. Natl. Acad. Sci. U.S.A.* **2005**, *102*, 5315–5322.
(4) Ilan, B.; Berne, B. J.; Flynn, G. W. *J. Phys. Chem. C* **2007**, *111*, 18243–18250.
(5) Florio, G. M.; Werblowsky, T. L.; Muller, T.; Berne, B. J.; Flynn, G. W. *J. Phys. Chem. B* **2005**, *109*, 4520–4532.
(6) Krishnan, M.; Balasubramanian, S.; Clarke, S. *J. Chem. Phys.* **2003**, *118*, 5082–5086.
(7) Hentschke, R.; Schurmann, B. L.; Rabe, J. P. *J. Chem. Phys.* **1992**, *96*, 6213–6221.
(8) Hansen, F. Y.; Herwig, K. W.; Matthies, B.; Taub, H. *Phys. Rev. Lett.* **1999**, *83*, 2362–2365.
(9) Claypool, C. L.; Faglioni, F.; Goddard, W. A.; Gray, H. B.; Lewis, N. S.; Marcus, R. A. *J. Phys. Chem. B* **1997**, *101*, 5978–5995.
(10) Tomanek, D.; Louie, S. G.; Mamin, H. J.; Abraham, D. W.; Thomson, R. E.; Ganz, E.; Clarke, J. *Phys. Rev. B* **1987**, *35*, 7790–7793.
(11) Giancarlo, L. C.; Flynn, G. W. *Annu. Rev. Phys. Chem.* **1998**, *49*, 297–336.
(12) Tomanek, D.; Louie, S. G. *Phys. Rev. B* **1988**, *37*, 8327–8336.
(13) Fisher, A. J.; Blochl, P. E. *Phys. Rev. Lett.* **1993**, *70*, 3263–3266.
(14) Seo, D. K.; Ren, J.; Whangbo, M. H. *Surf. Sci.* **1997**, *370*, 252–258.
(15) Kim, K.; Plass, K. E.; Matzger, A. J. *Langmuir* **2003**, *19*, 7149–7152.
(16) Plass, K. E.; Matzger, A. J. *Chem. Commun.* **2006**, 3486–3488.
(17) Lei, S. B.; Wang, C.; Fan, X. L.; Wan, L. J.; Bai, C. L. *Langmuir* **2003**, *19*, 9759–9763.
(18) Yang, Y. L.; Deng, K.; Zeng, Q. D.; Wang, C. *Surf. Interface Anal.* **2006**, *38*, 1039–1046.
(19) Cyr, D. M.; Venkataraman, B.; Flynn, G. W. *Chem. Mater.* **1996**, *8*, 1600–1615.
(20) Wintgens, D.; Yablon, D. G.; Flynn, G. W. *J. Phys. Chem. B* **2003**, *107*, 173–179.
(21) Kim, K. B.; Plass, K. E.; Matzger, A. J. *Langmuir* **2005**, *21*, 647–655.
(22) Kim, K.; Matzger, A. J. *J. Am. Chem. Soc.* **2002**, *124*, 8772–8773.
(23) De Feyter, S.; De Schryver, F. C. *J. Phys. Chem. B* **2005**, *109*, 4290–4302.
(24) McGonigal, G. C.; Bernhardt, R. H.; Thomson, D. J. *Appl. Phys. Lett.* **1990**, *57*, 28–30.
(25) Nath, K. G.; Ivasenko, O.; MacLeod, J. M.; Miwa, J. A.; Wuest, J. D.; Nanci, A.; Perepichka, D. F.; Rosei, F. *J. Phys. Chem. C* **2007**, *111*, 16996–17007.
(26) Rabe, J. P.; Buchholz, S.; Askadskaya, L. *Phys. Scr.* **1993**, *T49A*, 260–263.
(27) Krishnan, M.; Balasubramanian, S.; Clarke, S. *Proc. - Indian Acad. Sci., Chem. Sci.* **2003**, *115*, 663–677.
(28) Ilan, B. F. G. M.; Müller, T.; Werblowsky, T. L.; Hybertsen, M.; Berne, B. J.; Flynn, G. W. Unpublished work, 2008.
(29) Liang, W.; Whangbo, M. H.; Wawkuschewski, A.; Cantow, H. J.; Magonov, S. N. *Adv. Mater.* **1993**, *5*, 817–821.
(30) Udier-Blagovic, M.; De Tirado, P. M.; Pearlman, S. A.; Jorgensen, W. L. *J. Comput. Chem.* **2004**, *25*, 1322–1332.
(31) Stern, H. A.; Xu H.; Harder, E.; Rittner, F.; Pavese, M.; Berne, J. B. Unpublished work, 2008.
(32) Steele, W. A. *Surf. Sci.* **1973**, *36*, 317–352.
(33) Soler, J. M.; Artacho, E.; Gale, J. D.; Garcia, A.; Junquera, J.; Ordejon, P.; Sanchez-Portal, D. *J. Phys.: Condens. Matter* **2002**, *14*, 2745–2779.
(34) Hohenberg, P.; Kohn, W. *Phys. Rev. B* **1964**, *136*, B864–B871.
(35) Ceperley, D. M.; Alder, B. J. *Phys. Rev. Lett.* **1980**, *45*, 566–569.
(36) Perdew, J. P.; Zunger, A. *Phys. Rev. B* **1981**, *23*, 5048–5079.
(37) Troullier, N.; Martins, J. L. *Phys. Rev. B* **1991**, *43*, 1993–2006.
(38) Monkhorst, H. J.; Pack, J. D. *Phys. Rev. B* **1976**, *13*, 5188–5192.
(39) Tersoff, J.; Hamann, D. R. *Phys. Rev. B* **1985**, *31*, 805–813.
(40) Groszek, A. J. *Proc. R. Soc. London, Ser. A* **1970**, *314*, 473–498.
(41) Kitaigorodskii, A. I. *Molecular crystals and molecules*; Academic Press: New York, 1973.
(42) Rabe, J. P.; Buchholz, S. *Science* **1991**, *253*, 424–427.
(43) Herwig, K. W.; Matthies, B.; Taub, H. *Phys. Rev. Lett.* **1995**, *75*, 3154.
(44) Yang, T.; Berber, S.; Liu, J.-F.; Miller, G. P.; Tomanek, D. *J. Chem. Phys.* **2008**, *128*, 124709–8.

NL8014186